

Development of Nano-Structured AA1050 by ECAE and Thermal Treatments

Carmelo J. Luis*, Javier León, Rodrigo Luri, Ignacio Puertas, Ivan Pérez, Daniel Salcedo

Department of Mechanical, Energetics and Materials Engineering, Public University of Navarre, Pamplona, Spain.
Email: *cluis.perez@unavarra.es

Received July 22nd, 2011; revised September 12th, 2011; accepted September 22nd, 2011.

ABSTRACT

In this present work, a study regarding the change in the mechanical properties and in the microstructure of the aluminium alloy AA1050 is made after being processed by severe plastic deformation (SPD) with Equal Channel Angular Extrusion (ECAE). Optical and scanning electron microscopy techniques will be employed in order to determine the evolution of the microstructure after different thermal treatments, subsequent to the severe plastic deformation process. This present work involves a profound study on the change in the mechanical properties for an alloy which has a very low value of strain hardening at room temperature. With this, it is demonstrated that it is possible to improve its mechanical properties significantly with an adequate combination of ECAE processing and thermal treatments.

Keywords: ECAE, SPD, Aluminium, UFG

1. Introduction

In these days, there is a great deal of interest in the manufacturing of ultrafine grained (UFG) materials either for research or commercial purpose. One of the most interesting techniques for their obtention is severe plastic deformation (SPD), as can be shown in studies such as that from Furukawa *et al.* [1]. In the state-of-the-art study made by Valiev *et al.* [2], different techniques are outlined in order to produce high values of plastic deformation, such as: ECAE, HPT and ARB, among others, severe plastic deformation (SPD) being a favorable method to conform and to control the mechanical behavior of the materials.

In this present work, the so-called Extrusion Channel Angular Extrusion (ECAE) is employed. This process consists in a severe plastic deformation (SPD) process, which was initially developed by V. M. Segal *et al.* [3] in the former Soviet Union. The ECAE process, as is shown in studies such as that from González *et al.* [4], consists in performing an extrusion through a die which has two channels with the same cross-section that intersect at an angle, generally varying between 90° y 135° (as can be observed in **Figure 1**). When the material is extruded through the intersection between both channels of the die is mainly deformed by a shear strain mechanism in the presence of a high hydrostatic pressure imposed by the ECAE die. This restriction avoids the material fracture

and it allows the material to be deformed up to much higher values than those which are possible to achieve with conventional thermo-mechanical processes.

The ECAE process has been applied to a large number of materials. In the study from N. Lugo *et al.* [5], the mechanical properties for the processing of copper billets were improved and thus, a grain refinement was obtained. Furthermore, satisfactory results were attained in materials such as titanium processed at room temperature [6]. Other authors analyze different processing strategies in order to achieve high strain rate superplasticity in magnesium alloys [7]. Nevertheless, aluminium alloys are the most widely studied materials [8]. Relevant improvements are found in mechanical properties such as the tensile strength and the hardness [9,10], the conformability [11] and the creep behavior [12].

With respect to the mechanisms which are responsible for the microstructural modification in these alloys, there exist a large number of studies in the bibliography such as [13-15], among others. Moreover, other studies can be found in which they analyze the use of several process configurations that affect the extrusion channel angle or the processing route [16], comparisons with traditional thermo-mechanical methods or variations on the original process, such as BP-ECAP (back pressure-ECAE) [17]. Nevertheless, as far as is known, the number of studies related to the change in the mechanical properties after

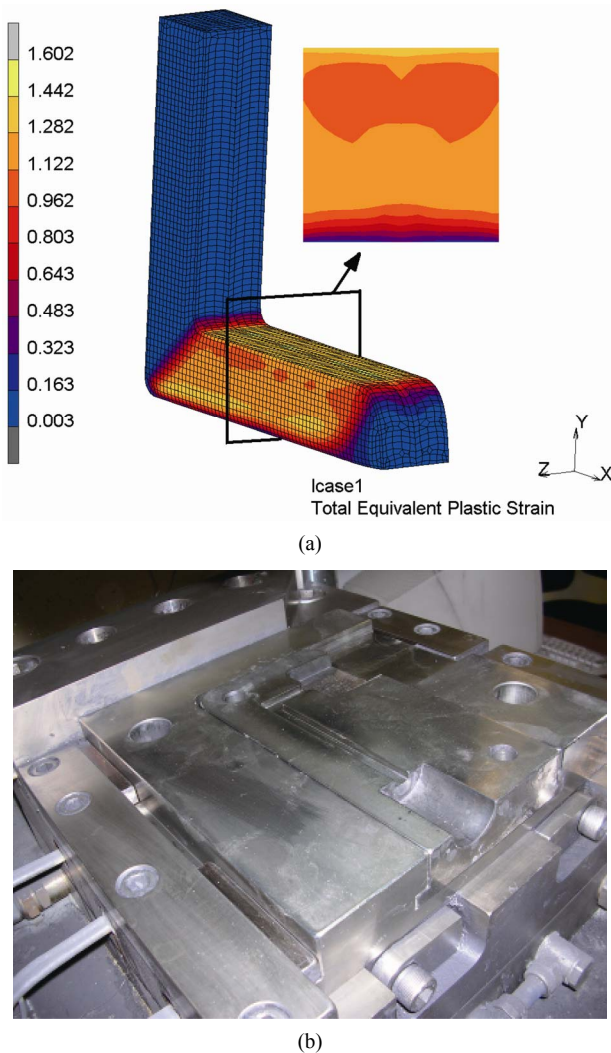


Figure 1. (a) FEM simulation of the ECAE process and (b) the ECAE Press.

different thermal treatments is not very high. In this present study, it is shown that it is possible to obtain materials with a grain size in the submicrometric or even nanometric range with a significant improvement in its mechanical properties by means of combining a low number of ECAE passages (using with route C) and adequate thermal treatments

2. Set-up of the Experimentation

The aluminium alloy AA1050 was processed by ECAE at room temperature with an extrusion hydraulic press, developed by the Research Group in Materials and Manufacturing Engineering from the Public University of Navarre, as can be observed in **Figure 1**. The extrusion velocity employed in all the tests was 50 mm/min. The cross-section of the aluminium billets was a square of 9 mm by 9 mm and their length was 80 mm. The lubricant

used to perform the ECAE process was MoS₂.

When the same billet is processed by ECAE several times, different routes can be used [4,18]. In this case route C was selected. This route consists in rotating the billet 180°, around its longitudinal axis, before it is introduced at the entrance channel of the die to perform a new passage. In this way, a great deal of homogeneity in the deformation value along the cross-section of the billets is achieved, after having completed an even number of passages.

There are different types of geometry dies cited in the bibliography. The most used in the past provided an outer radius which was not tangential to the walls of the die channel. Subsequently, some other improved geometries have been developed, such as those by Luis [19] and Luri *et al.* [20], which put forward the use of external and internal radii both tangential to the walls of the die channel. In recent published works, the authors have shown that traditional ECAE dies should be replaced by these latter dies which allow us to obtain higher deformation values at the same time that the imparted damage is reduced [21]. These dies are those which have been utilized in this present study. In this case, a geometry with equal radii has been employed, with both the external and the internal radii being of 1.95 mm.

Each of the microhardness (HV) values was assessed from ten random measurements throughout the cross-section of the samples. The cycle of each indentation is composed of a charging time of 3 s, 10 s of maintaining charge and 3 s of discharge with an indentation force of 3 N.

Three tensile tension tests were performed for each particular case at a velocity of 100 N/s. The employed billets were machined starting from a initial square cross-section of 9 mm by 9 mm down to a diameter of 5 mm in the necking zone.

To carry out the microscopy study, the samples were cut using a metallographic saw equipped with a silicon carbide (SiC) disk. Subsequently, they were mounted in a non-conductive acrylic resin and they were sanded down with different grain size sandpapers and polished with cloths, using diamond and colloidal silica as abrasives. To perform the optical microscopy, the Barker electrolytic etching was utilised since it allows us to observe the microstructure under polarized light. In the case of the scanning electron microscopy, an electropolishing by a solution of perchloric acid and ethanol was carried out. The equipment used was a high resolution field emission electronic microscope equipped with detectors of secondary and backscattered electrons along with electron backscattered diffraction (EBSD).

3. Mechanical Properties Analysis

Figure 2 shows the microhardness (HV) results of the

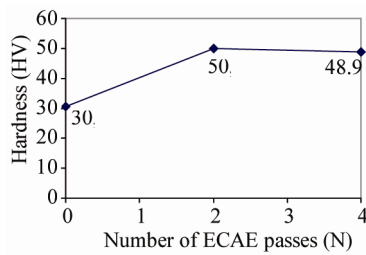


Figure 2. Microhardness (HV) of AA1050 for N = 0, N = 2 and N = 4.

starting material and after having been subjected it to two ECAE passages (N2) and to four ECAE passages (N4) with no thermal treatment.

The same occurs with the mechanical properties obtained from the tensile tension tests in such a way that the yield stress and the tensile strength increase and the elongation at break decreases after two passages, as can be seen in Figure 3. For the fourth passage (N = 4), it is obtained that the mechanical properties do not vary practically anything.

Table 1 shows a summary with the hardness measurements (expressed in Vickers hardness number) attained in the different samples and cases studied.

Figure 4 shows the hardness values of the starting material (N0) and the hardness values after two passages

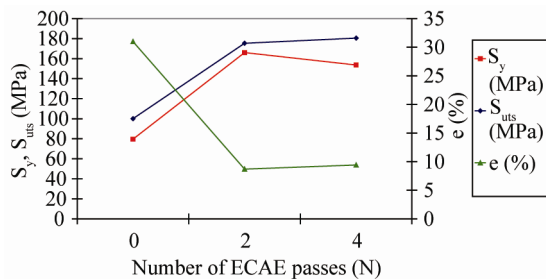


Figure 3. Variation in mechanical properties: S_y , S_{uts} y e (%) of the aluminium alloy AA1050 as a function of the number of ECAE passages.

Table 1. Microhardness values of AA1050.

Passage (N)	Temperature (°C)	Time (h)	Hardness (HV)
0			30.6
2			50.0
4			48.9
2	150	1	51.4
2	200	1	50.0
2	250	1	48.9
2	275	1	44.8
2	300	1	37.8
2	325	1	28.4
2	350	1	27.7

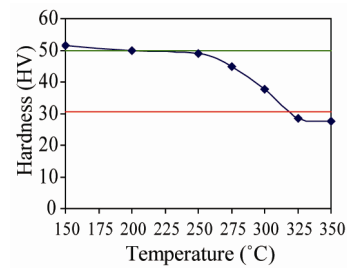


Figure 4. Microhardness (HV) of AA1050 (N = 2) after previous thermal treatments of 1 h at different values of temperature.

(N2) superimposed with those obtained from the different treatments. A gradual decrease in hardness is observed from 250°C upwards, this reaching a value lower than the initial one from 325°C.

Microhardness values and micrographs were carried out over the material processed and thermally treated at five different temperature values and with holding time values of 0 h, 0.5 h, 1 h, 1.5 h, 3 h, 5 h and 7 h. Figure 5 shows a summary with the variation in hardness for the latter treatments.

After carrying out this study, the thermal treatments at 250°C, 275°C and 300°C were selected. In the following sections, the results obtained with these treatments are outlined.

3.1. Thermal Treatment at 250°C

The optimum recovery temperature was considered to be that in which the ECAE processed aluminium alloy AA1050 undergoes a low drop in its hardness value along with an improvement in its ductility value, after being subjected to the specific thermal treatment. On the basis of the previously-shown thermal treatments, a temperature value of 250°C has been selected as the optimum treatment temperature. Table 2 and Figure 6 show how the AA1050 microhardness varies with this treat-

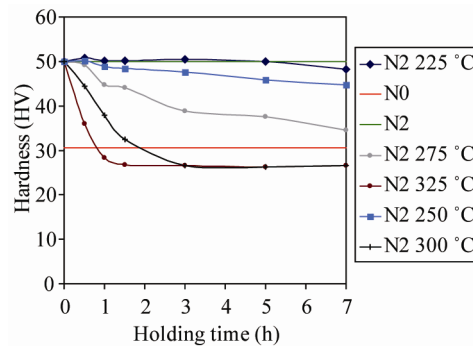
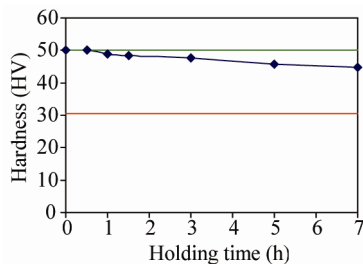


Figure 5. Microhardness (HV) of AA1050 N = 2 as a function of the holding time of the thermal treatment at 225°C, 250°C, 275°C, 300°C and 325°C.

Table 2. Microhardness (HV) of AA1050 after the thermal treatment at 250°C.

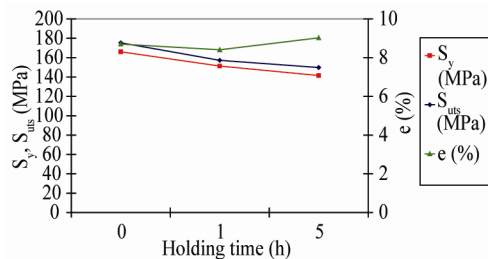
Passage (N)	Temperature (°C)	Time (h)	Hardness (HV)
2	250	0	50.0
2	250	0.5	50.2
2	250	1	48.9
2	250	1.5	48.4
2	250	3	47.6
2	250	5	45.8
2	250	7	44.7

**Figure 6. Microhardness (HV) of AA1050 (N = 2) as a function of the holding time of the recovery thermal treatment at 250°C.**

ment as a function of duration time.

As can be observed in **Table 2**, the material hardness does not undergo a significant drop in relation to the treatment duration time, even for the thermal treatment of 7 h. In order to analyze other material mechanical properties, such as the yield stress (S_y), the tensile strength (S_{uts}) and the ductility (e), billets were machined from the material ECAE processed and then subjected to subsequent thermal treatments. Then, tensile tension tests were carried out and the three following duration time values were selected for the thermal treatment: 0 h, 1 h and 5 h.

As can be observed in **Figure 7**, not only the yield stress but also the tensile strength of the material decrease with respect to the duration time of the recovery thermal treatment. Thus, values of decrease in the tensile strength of 10.4% and 14.6% can be evaluated in relation

**Figure 7. Variation in the AA1050 mechanical properties (N = 2): S_y , S_{uts} and e as a function of the holding time of the recovery thermal treatment at 250°C.**

to the selected thermal treatment holding time values of 1 h and 5 h, respectively. On the other hand, as could be expected, an improvement in the ductility of the treated material ($t = 5$ h) of 3.7% is achieved in comparison with the material processed twice by ECAE ($N = 2$).

3.2. Thermal Treatment at 275°C

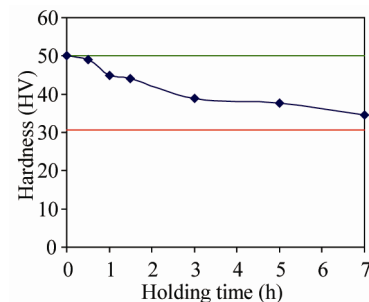
The temperature of this thermal treatment has been selected so that the aluminium alloy remains at an intermediate stage between recovery and recrystallization. At first, **Table 3** and **Figure 8** show the variation in microhardness for the aluminium alloy AA1050 as a function of the duration time of this present thermal treatment.

It can be observed that the microhardness value progressively decreases down to a value very close to the starting material hardness. In this way, three duration time values: 0 h, 1 h and 5 h were selected so as to obtain information by means of the tensile tension tests.

As can be observed in **Figure 9**, not only the yield stress but also the tensile strength of the material decrease when the thermal treatment holding time is increased. Thus, decreasing values for the yield stress of 16.5% and 33.9%, respectively, can be assessed with respect to the selected thermal treatment duration time values of 1 h and 5 h. The tensile strength also decreases percentage values of 17.4% and 31.8%, respectively. On the other hand, as might be expected, an improvement in the ductility of the thermally-treated material of 3.5% (t

Table 3. Microhardness (HV) of AA1050 after the thermal treatment at 275°C.

Passage (N)	Temperature (°C)	Time (h)	Hardness (HV)
2	275	0	50.0
2	275	0.5	49.1
2	275	1	44.8
2	275	1.5	44.1
2	275	3	38.9
2	275	5	37.6
2	275	7	34.6

**Figure 8. Microhardness (HV) of AA1050 (N = 2) as a function of the holding time of the thermal treatment at 27°C.**

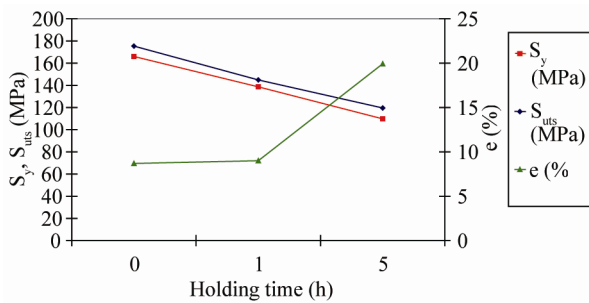


Figure 9. Variation in the AA1050 mechanical properties ($N = 2$): S_y , S_{uts} and e as a function of the holding time of the thermal treatment at 275°C.

= 1 h) and 129% (t = 5 h) is achieved in relation to the material processed twice by ECAE ($N = 2$).

3.3. Thermal Treatment at 300°C

The temperature value of 300°C is chosen so as to make the recrystallization study more controllable since a too high temperature value is used, the recrystallization process and thus the decrease in hardness become too rapid. As can be observed in **Table 4** and **Figure 10**, the microhardness value decreases in a controllable way up to a time of 3 h and subsequently, it remains at a lower value than that from the starting material.

In the same way as in the earlier cases, in order to find how the ductility and the tensile strength vary, diverse tensile tension tests were performed. The obtained results

Table 4. Microhardness (HV) of AA1050 after the thermal treatment at 300°C.

Passage (N)	Temperature (°C)	Time (h)	Microhardness (HV)
2	300	0	50.0
2	300	0.5	44.4
2	300	1	37.8
2	300	1.5	32.4
2	300	3	26.6
2	300	5	26.3
2	300	7	26.6

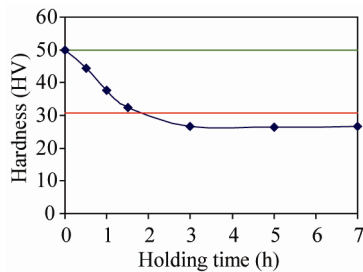


Figure 10. Microhardness (HV) of AA1050 ($N = 2$) as a function of the holding time of the recrystallization thermal treatment at 300°C.

from these tests are shown in **Figure 11**.

As can be observed, not only the yield stress of the material but also its tensile strength diminishes considerably. As in the previous sections, values of decrease in the yield stress of 33% and 67.1%, respectively, can be evaluated for selected thermal treatment duration time values of 1 h and 5 h. Similarly, the tensile strength also decreases in a percentage of 31.1% and 44.5%, respectively. Regarding the ductility of the thermally-treated material, an improvement of 114.8% and 376% is observed in the cases of the thermal treatments with a duration time of 1 h and 5 h, respectively, in comparison with the material processed twice by ECAE ($N = 2$).

4. Microstructure Analysis

With the aim of analyzing the microstructural changes in the processed material for the different selected thermal treatments, diverse optical and SEM micrographs along with EBSD mappings and their corresponding distribution functions for grain size and aspect ratio are depicted in **Figures 12-23**. As can be observed, as the material is being processed by ECAE, the present microstructure goes being replaced by a new submicrometric and nanometric structure lattice due to the introduction of a high dislocations density into the material. The subgrains of this new lattice are of a lower size and they possess a more equiaxial morphology than the initial grains (see **Table 5**). This fact becomes evident when the SEM

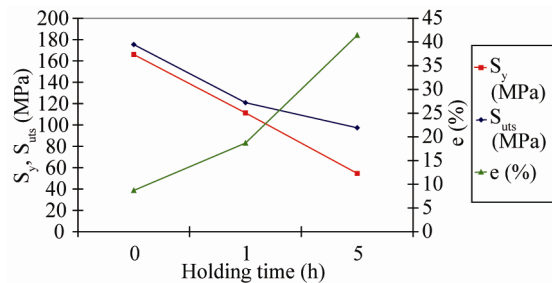


Figure 11. Variation in the AA1050 mechanical properties ($N = 2$): S_y , S_{uts} and e as a function of the holding time of the recrystallization thermal treatment at 300°C.

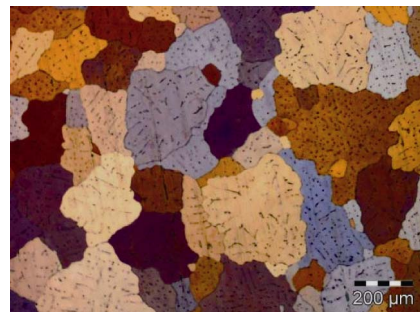


Figure 12. N0 state (starting material).

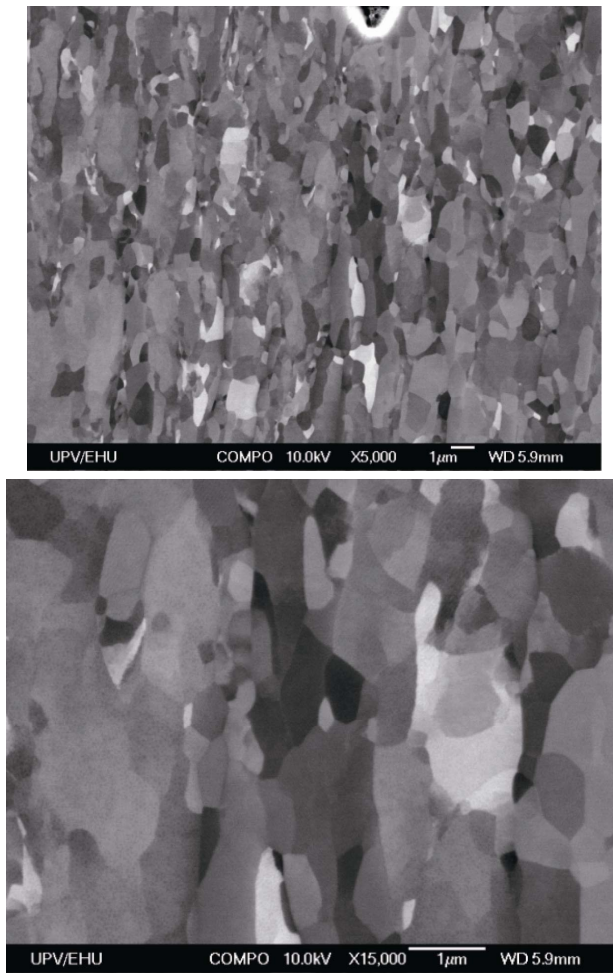


Figure 13. N2 state (material processed twice by ECAE with route C).

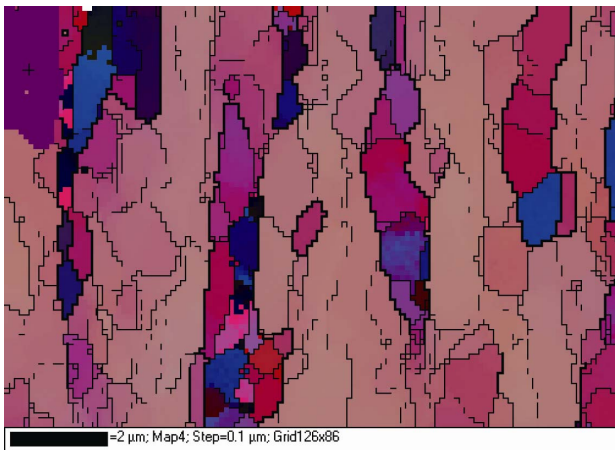


Figure 14. EBSD over the material processed by ECAE up to N2.

micrographs for the aluminium alloy AA1050 are observed, as is shown in **Figure 13**, **Figure 16**, **Figure**

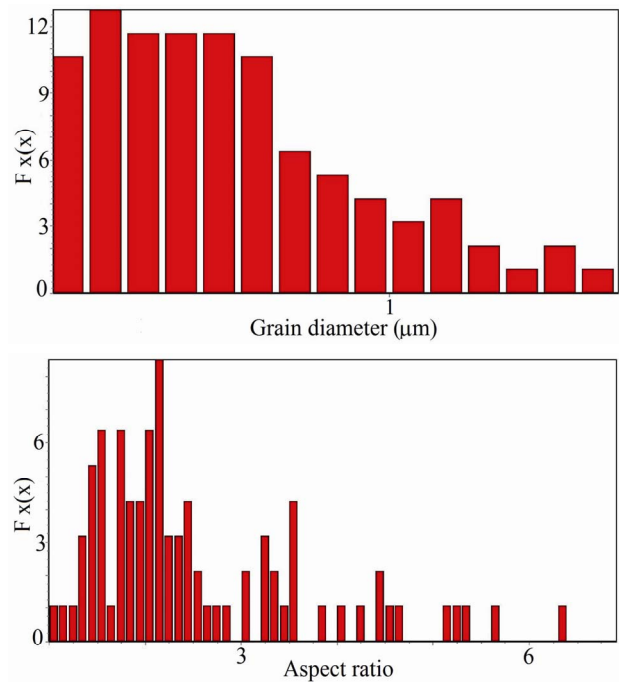


Figure 15. Distribution function for grain size and aspect ratio (ECAE, N2).

Table 5. Grain size and aspect ratio for the different AA1050 deformation states.

Deformation state	Grain size (μm)	Aspect ratio
N0	≈ 250	> 5
N2	0.60 ± 0.35	2.46 ± 1.26
N4	0.65 ± 0.37	2.41 ± 1.20
N2 + recovery	0.54 ± 0.32	2.25 ± 1.16
NN2	0.84 ± 0.49	2.37 ± 1.13

19 and **Figure 21**. In these figures, not only a preferential directionality in the material flow can be observed but also a certain level of heterogeneity in the grain size values, which vary from $1 \mu\text{m}$ down to values even of 100 nm and 200 nm . This leads to a significant structure refinement since the grain size of the starting material is found to be between $200 \mu\text{m}$ and $300 \mu\text{m}$ (see **Figure 12**).

Table 5 shows the mean value of the subgrains after the processing is approximately $0.6 \mu\text{m}$ as opposed to the value of $250 \mu\text{m}$ for the non-processed material, which implies a reduction of more than 400 times in relation to its original size grain.

The most significant differences obtained when comparing the different states of the ECAE processed material are found by observing the EBSD mappings of N2 and N4 states (see **Figure 14** and **Figure 17**) and their corresponding distribution functions for the grain size

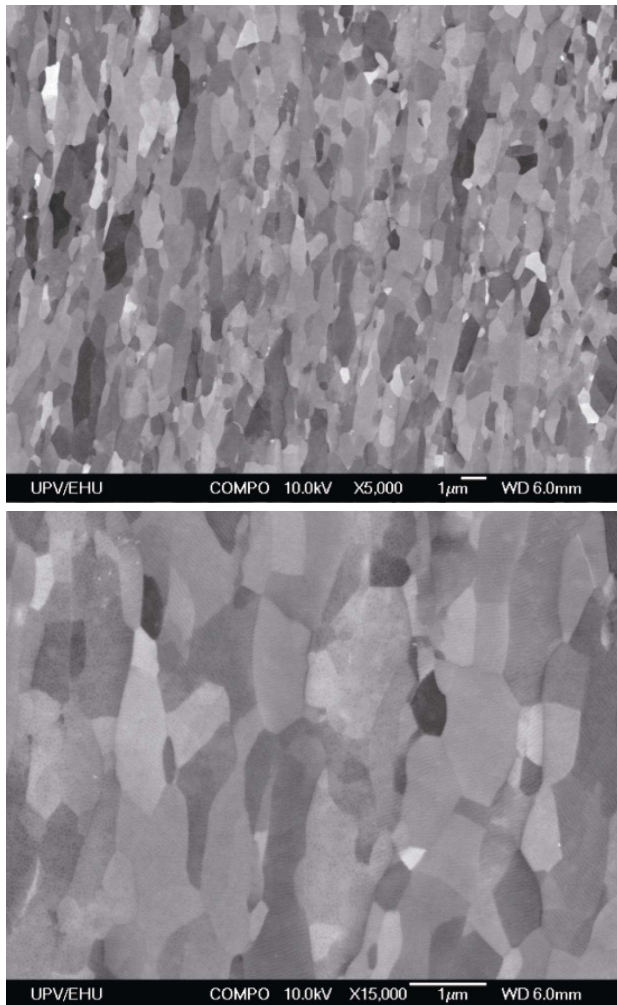


Figure 16. N4 state (material processed four times by ECAE with route C).

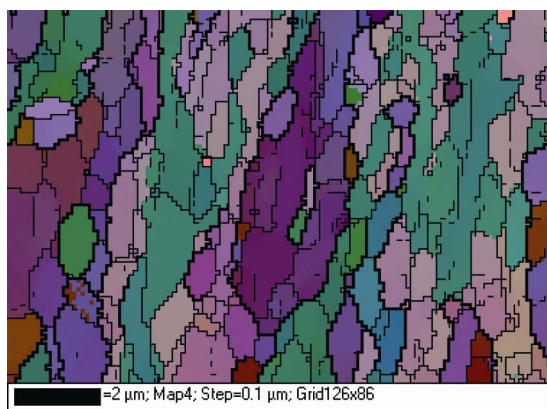


Figure 17. EBSD over the material processed by ECAE up to N4.

and the aspect ratio (see **Figure 15** and **Figure 18**). In the samples processed up to four passages, grain bounda-

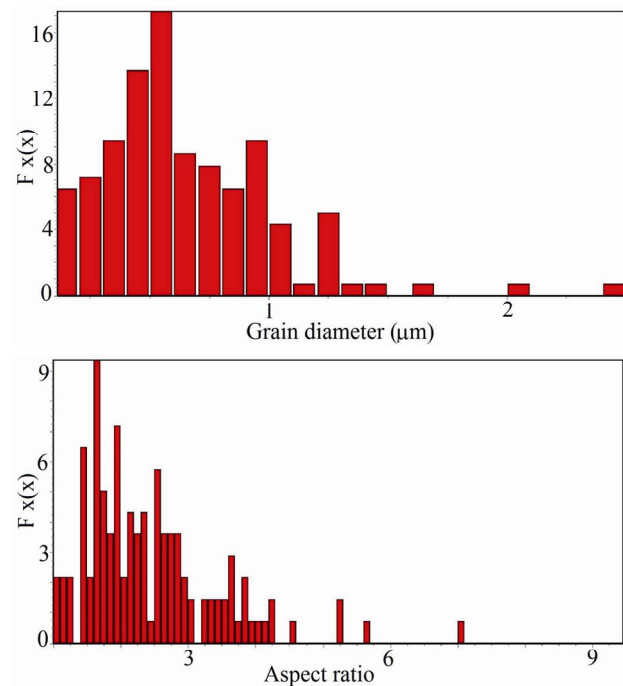


Figure 18. Distribution function for grain size and aspect ratio (ECAE, N4).

ries are found to be sharper and with a higher level of misorientation than in the case of N2. This is due to the fact that the higher level of dislocations density introduced in the material has caused a higher misorientation value between the material microstructure subgrains and thus an increase in the high angle boundaries (HAB,s). This point is in agreement with the typical microstructure evolution in materials processed by severe plastic deformation with ECAE.

The aspect ratio, which provides a measurement of the equiaxiality for the microstructure grains, shows that there exist improvements after the ECAE processing, where this aspect ratio is higher than 5 for the non-processed material grains and it is reduced down to values close to 2.4, which means an improvement of more than 50%.

Figure 19 show several SEM micrographs at the recovery state after N2. As can be observed, there exists a more uniform grain distribution in relation to that obtained in the material after being processed by ECAE at room temperature and without heat treatment. Moreover, **Figure 20** shows a lower variation in the grain size distribution. It can be observed that there exist grains which range from 100 nm to 800 nm, with a lower variation than that observed in **Figure 18**.

Furthermore, AA1050 initial billets (N0) were processed twice by ECAE and after a subsequent recrystallization thermal treatment, they were again processed

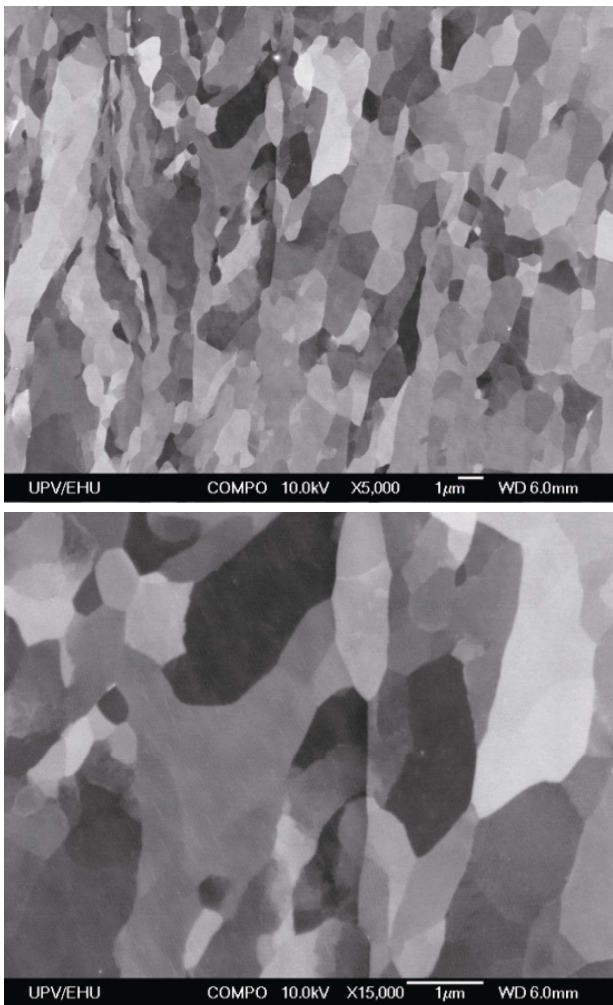


Figure 19. N2 state and subsequent recovery thermal treatment at 250°C during 5 h.

twice by ECAE, which is denominated as NN2. With this combination, it was intended to probe if the NN2 state was able to reduce not only the grain size but also the aspect ratio in relation to N2 and N4 states. However, as can be observed in **Table 5** and it is also shown in **Figures 21-23**, no improvement can be appreciated.

5. Conclusions

In this present study, the variation in mechanical properties and microstructure has been analysed for the aluminium alloy AA1050. It has been determined that it is possible to achieve a significant improvement in the mechanical properties and in the grain size of this material, either with or without the application of thermal treatments.

An outstanding refinement in the microstructure has been observed since the non-processed material grain size is found to be between 200 µm and 300 µm and after

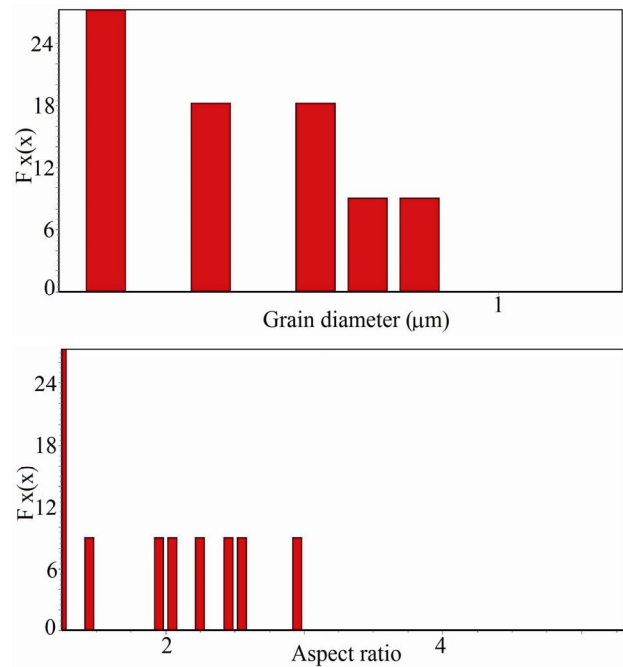


Figure 20. Distribution function for grain size and aspect ratio in the case of N2 state and subsequent recovery thermal treatment at 250°C during 5 h.

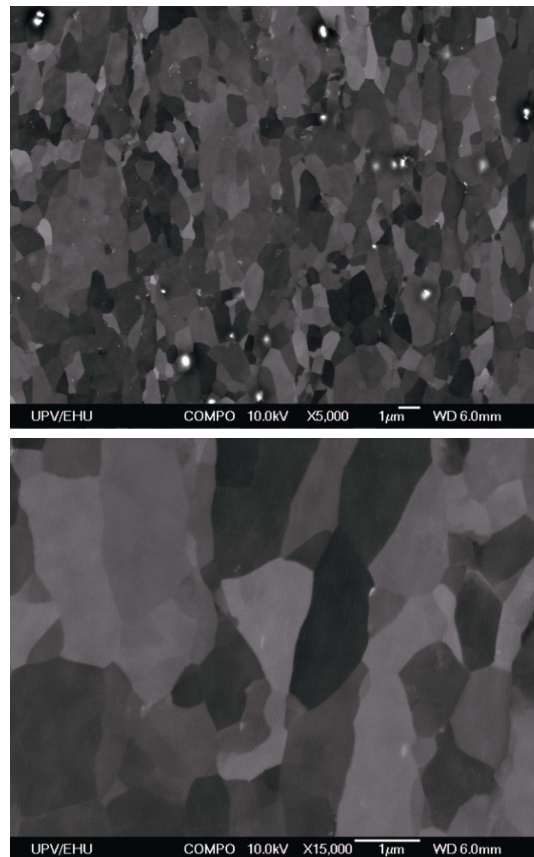


Figure 21. NN2 state.

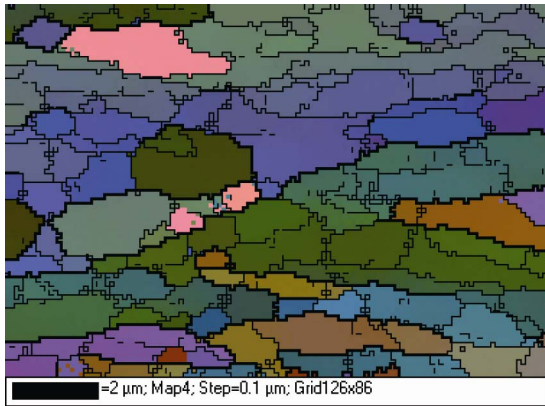


Figure 22. EBSD over the material processed by ECAE up to NN2.

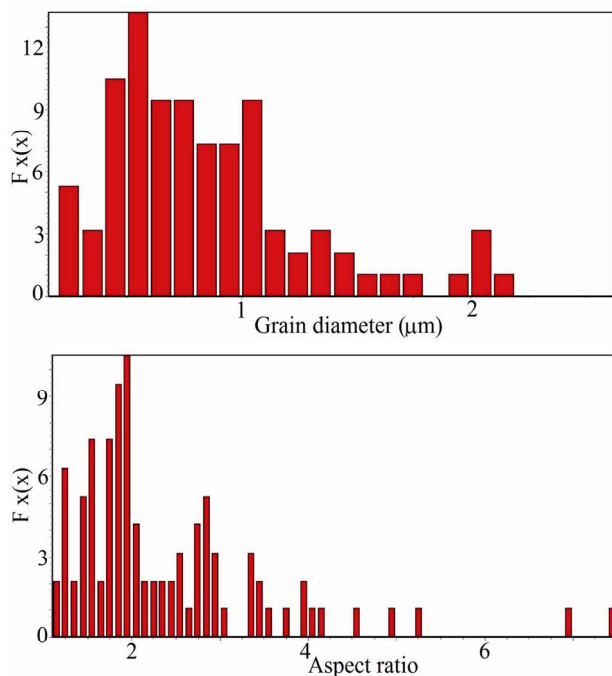


Figure 23. Distribution function for grain size and aspect ratio (ECAE, NN2).

being processed by ECAE, this has decreased approximately down to 600 nm.

Furthermore, it has been established that the thermal treatments of greater interest for the considered aluminium alloy are the three following ones. Firstly, a recovery thermal treatment at a temperature of 250°C during 5 hours, which is appropriated for applications in which good mechanical properties are required, also being able a slight improvement in ductility with respect to the processed material (N2 through route C). Secondly, a thermal treatment at 275°C during 1 hour, which is similar to the previous one but with an improvement in the elongation at break along with a slight worsening in the tensile

strength. Thirdly, a recrystallization thermal treatment at 300°C during 5 hours, which is remarkable for the improvement in the processed material ductility in relation to the initial one.

6. Acknowledgements

The authors of the present study acknowledge the support given by the Government of Navarre (Project EUROINNOVA NANOCONS-IIM10784.R11).

REFERENCES

- [1] M. Furukawa, Z. Horita, M. Nemoto, R. Z. Valiev and T. Langdon, "Microstructural Characteristics of an Ultrafine Grain Metal Processed with Equal-Channel Angular Pressing," *Materials Characterization*, Vol. 37, No. 5, 1996, pp. 277-283. [doi:10.1016/S1044-5803\(96\)00131-3](https://doi.org/10.1016/S1044-5803(96)00131-3)
- [2] R. Z. Valiev, A. V. Korznikov and R. R. Mulyukov, "Structure and Properties of Ultrafine-Grained Materials Produced by Severe Plastic Deformation," *Materials Science and Engineering: A*, Vol. 168, No. 2, 1993, pp. 141-148. [doi:10.1016/0921-5093\(93\)90717-S](https://doi.org/10.1016/0921-5093(93)90717-S)
- [3] V. M. Segal, "Plastic Working of Metals by Simple Shear," *Russian Metallurgy*, Vol. 1, 1981, pp. 99-105.
- [4] P. A. Gonzalez, C. Luis-Pérez, Y. Garcés and J. Gil-Sevillano, "ECAE, una Tecnología de Procesado Emergente Para Producir Propiedades Relevantes en Materiales Metálicos," *Revista de Metalurgia*, Vol. 37, No. 6, 2001, pp. 673-692.
- [5] N. Lugo, J. M. Cabrera, N. Llorca, C.J. Luis, R. Luri, J. León and I. Puertas, "Grain Refinement of Pure Copper by ECAP," *Materials Science Forum*, Vol. 584-586, 2008, pp. 393-398. [doi:10.4028/www.scientific.net/MSF.584-586.393](https://doi.org/10.4028/www.scientific.net/MSF.584-586.393)
- [6] X. Zhao, W. Fu, X. Yang and T. G. Langdon, "Microstructure and Properties of Pure Titanium Processed by Equal-Channel Angular Pressing at Room Temperature," *Scripta Materialia*, Vol. 59, No. 5, 2008, pp. 542-545. [doi:10.1016/j.scriptamat.2008.05.001](https://doi.org/10.1016/j.scriptamat.2008.05.001)
- [7] R. Figueiredo and T. G. Langdon, "Strategies for Achieving High Strain Rate Superplasticity in Magnesium Alloys Processed by Equal-Channel Angular Pressing," *Scripta Materialia*, Vol. 61, No. 1, 2009, pp. 84-87. [doi:10.1016/j.scriptamat.2009.03.012](https://doi.org/10.1016/j.scriptamat.2009.03.012)
- [8] R. Z. Valiev and T. G. Langdon, "Principles of Equal-Channel Angular Pressing as a Processing Tool for Grain Refinement," *Progress in Materials Science*, Vol. 51, No. 7, 2006, pp. 881-981. [doi:10.1016/j.pmatsci.2006.02.003](https://doi.org/10.1016/j.pmatsci.2006.02.003)
- [9] E. A. El-Danaf, "Mechanical Properties and Microstructure Evolution of 1050 Aluminum Severely Deformed by ECAP to 16 Passes," *Materials Science and Engineering: A*, Vol. 487, No. 1-2, 2008, pp. 189-200. [doi:10.1016/j.msea.2007.10.013](https://doi.org/10.1016/j.msea.2007.10.013)
- [10] C. Y. Yu, P.L. Sun, P. W. Kao and C. P. Chang, "Mechanical Properties of Submicron-Grained Aluminum," *Scripta Materialia*, Vol. 52, No. 5, 2005, pp. 359-363. [doi:10.1016/j.scriptamat.2004.10.035](https://doi.org/10.1016/j.scriptamat.2004.10.035)

- [11] A. Sivaraman and U. Chakkingal, "Investigations on Workability of Commercial Purity Aluminum Processed by Equal Channel Angular Pressing," *Journal of Materials Processing Technology*, Vol. 202, No. 1-3, 2008, pp. 543-548. [doi:10.1016/j.jmatprotec.2007.10.006](https://doi.org/10.1016/j.jmatprotec.2007.10.006)
- [12] M. Kawasaki, I. J. Beyerlein, S. C. Vogel and T. G. Langdon, "Characterization of Creep Properties and Creep Textures in Pure Aluminum Processed by Equal-Channel Angular Pressing," *Acta Materialia*, Vol. 56, No. 10, 2008, pp. 2307-2317. [doi:10.1016/j.actamat.2008.01.023](https://doi.org/10.1016/j.actamat.2008.01.023)
- [13] M. Kawasaki, Z. Horita and T. G. Langdon, "Microstructural Evolution in High Purity Aluminum Processed by ECAP," *Materials Science and Engineering: A*, Vol. 524, No. 1-2, 2009, pp. 143-150. [doi:10.1016/j.msea.2009.06.032](https://doi.org/10.1016/j.msea.2009.06.032)
- [14] J. May, H. W. Höppel and M. Göken, "Strain Rate Sensitivity of Ultrafine-Grained Aluminium Processed by Severe Plastic Deformation," *Scripta Materialia*, Vol. 53, No. 2, 2005, pp. 189-194. [doi:10.1016/j.scriptamat.2005.03.043](https://doi.org/10.1016/j.scriptamat.2005.03.043)
- [15] O. V. Mishin, J. R. Bowen and S. Lathabai, "Quantification of Microstructure Refinement in Aluminium Deformed by Equal Channel Angular Extrusion: Route A vs. Route Be in a 90 Degrees Die," *Scripta Materialia*, Vol. 63, No. 1, 2010, pp. 20-23. [doi:10.1016/j.scriptamat.2010.02.042](https://doi.org/10.1016/j.scriptamat.2010.02.042)
- [16] K. J. Kim, D. Y. Yang and J. W. Yoon, "Investigation of Microstructure Characteristics of Commercially Pure Aluminum during Equal Channel Angular Extrusion," *Materials Science and Engineering: A*, Vol. 485, No. 1-2, 2008, pp. 621-626.
- [17] K. Xia and X. Wu, "Back Pressure Equal Channel Angular Consolidation of Pure Al Particles," *Scripta Materialia*, Vol. 53, No. 11, 2005, pp. 1225-1229. [doi:10.1016/j.scriptamat.2005.08.012](https://doi.org/10.1016/j.scriptamat.2005.08.012)
- [18] Y. W. Tham, M. W. Fu, H. H. Hng, Q. X. Pei and K. B. Lim, "Microstructure and Properties of Al-6061 Alloy by Equal Channel Angular Extrusion for 16 Passes," *Materials and Manufacturing Processes*, Vol. 22, No. 7-8, 2007, pp. 819-824. [doi:10.1080/10426910701446754](https://doi.org/10.1080/10426910701446754)
- [19] C. J. Luis Pérez, "On the Correct Selection of the Channel Die in ECAP Processes," *Scripta Materialia*, Vol. 50, No. 3, 2004, pp. 387-393. [doi:10.1016/j.scriptamat.2003.10.007](https://doi.org/10.1016/j.scriptamat.2003.10.007)
- [20] R. Luri, C. J. Luis, J. León and M. A. Sebastián, "A New Configuration for Equal Channel Angular Extrusion Dies," *Journal of Manufacturing Science and Engineering-Transactions of the ASME*, Vol. 128, No. 4, 2006, pp. 860-865. [doi:10.1115/1.2194555](https://doi.org/10.1115/1.2194555)
- [21] R. Luri, C. J. Luis Pérez, D. Salcedo, I. Puertas, J. León, I. Pérez and J. P. Fuertes, "Evolution of Damage in AA-5083 Processed by Equal Channel Angular Extrusion Using Different Die Geometries," *Journal of Materials Processing Technology*, Vol. 211, No. 1, 2011, pp. 48-56. [doi:10.1016/j.jmatprotec.2010.08.032](https://doi.org/10.1016/j.jmatprotec.2010.08.032)